



Enhanced conductivity of aluminum doped ZnO films by hydrogen plasma treatment

H.P. Chang, F.H. Wang*, J.Y. Wu, C.Y. Kung, H.W. Liu

Department of Electrical Engineering and Graduate Institute of Optoelectronic Engineering, National Chung Hsing University, Taichung 402, Taiwan, ROC

ARTICLE INFO

Available online 10 May 2010

Keywords:

Aluminum doped zinc oxide (AZO)
Hydrogen plasma
Magnetron sputtering
Resistivity

ABSTRACT

Aluminum doped zinc oxide (AZO) thin films prepared by radio-frequency (RF) magnetron sputtering at various RF power were treated by hydrogen plasma to enhance the characteristics for transparent electrode applications. The hydrogen plasma treatment was carried out at 300 °C in a plasma enhanced chemical vapor deposition system. X-ray diffraction analysis shows that all AZO films have a (002) preferred orientation and film crystallinity seems no significant change after plasma treatment. The plasma treatment not only significantly decreases film resistivity but enhances electrical stability as aging in air ambient. The improved electrical properties are due to desorption of weakly bonded oxygen species, formation of Zn–H type species and passivation of deep-level defects during plasma treatment.

© 2010 Elsevier B.V. All rights reserved.

1. Introduction

Transparent conductive oxide (TCO) films have been applied extensively in optoelectronic devices because of their high visible transmittance and low resistivity [1,2]. Indium–tin–oxide (ITO) films are widely used in various TCO film applications, such as electro-optical devices, liquid crystal display devices, transparent electromagnetic shielding materials and unbreakable heat-reflecting mirrors. Aluminum doped zinc oxide (AZO) is a potential alternative to ITO because it is inexpensive and non-toxic as well as it exhibits good stability in plasma [3]. Moreover, a comparison with ITO films shows that AZO films can be deposited at low temperature and have good electrical conductivity and optical transmittance [1–3]. In recent years, extensive researches into AZO thin films have been performed and have been applied as transparent electrodes in flexible displays, plasma display panels, organic light emitting diode displays and solar cells [4–8].

The conductivity of the AZO thin film can be improved by increasing the crystallinity and vacancy content [9,10]. Furthermore, hydrogen in zinc oxide (ZnO) films can also form shallow donor to enhance the electrical property [11]. The effects of in-situ hydrogen doping and post-deposition annealing in hydrogen or vacuum on the structural, electrical and optical properties of AZO thin films were investigated [12–15]. Researchers investigate the effects of RF power and post-deposition annealing on the structural, electrical and optical properties of AZO thin films [12–16]. Methods to improve electrical properties such as post-deposition annealing treatment have been developed. Post-deposition annealing could reduce resistivity and cause a blue shift absorption edge in the transmission spectra of AZO

thin films. However, post-treatment must be implemented at high annealing temperature during long treatment time [12]. In addition, for post-annealing in a vacuum, the electrical conductivity increases with the increase of the substrate temperature. Oxygen vacancies in the crystal act as electron donors to improve the electrical properties of the thin film [9–11]. However, for large-area transparent electrode applications, the effects of hydrogen plasma treatment using plasma enhanced chemical vapor deposition (PECVD) system on the electrical properties of AZO thin films have not been investigated in detail

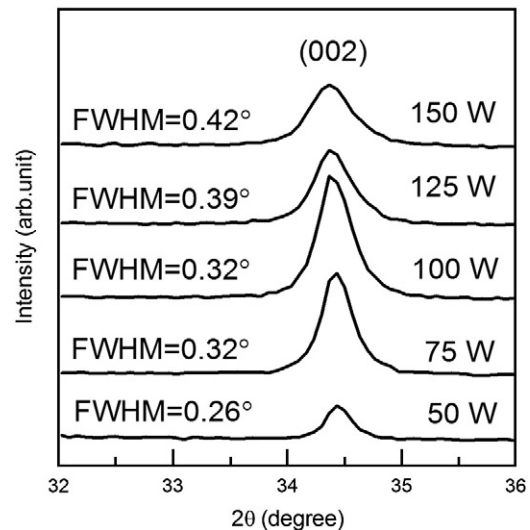


Fig. 1. X-ray diffraction patterns for AZO films deposited at various RF power.

* Corresponding author.

E-mail address: fansen@dragon.nchu.edu.tw (F.H. Wang).

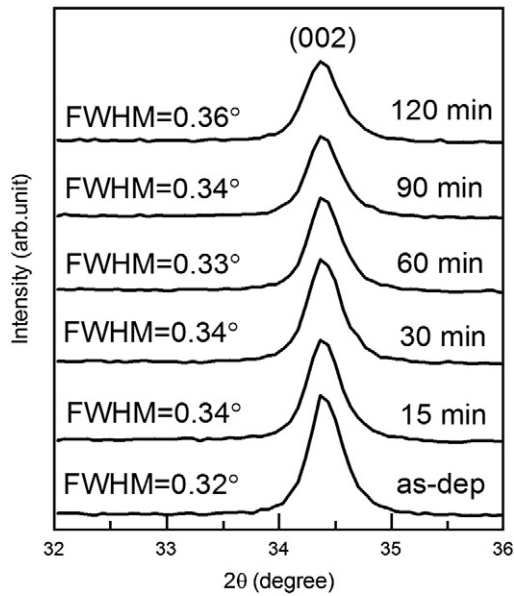


Fig. 2. X-ray diffraction patterns for AZO films deposited at RF power of 100 W with or without further plasma treatment at 300 °C for various times.

[16,17]. This work studies the effects of the plasma power and treatment duration on the electrical characteristics.

2. Experimental details

Zinc oxide powder mixed with 2 wt.% aluminum oxide was formed as a disc with a diameter of 2 in. and sintered to be used as a sputter

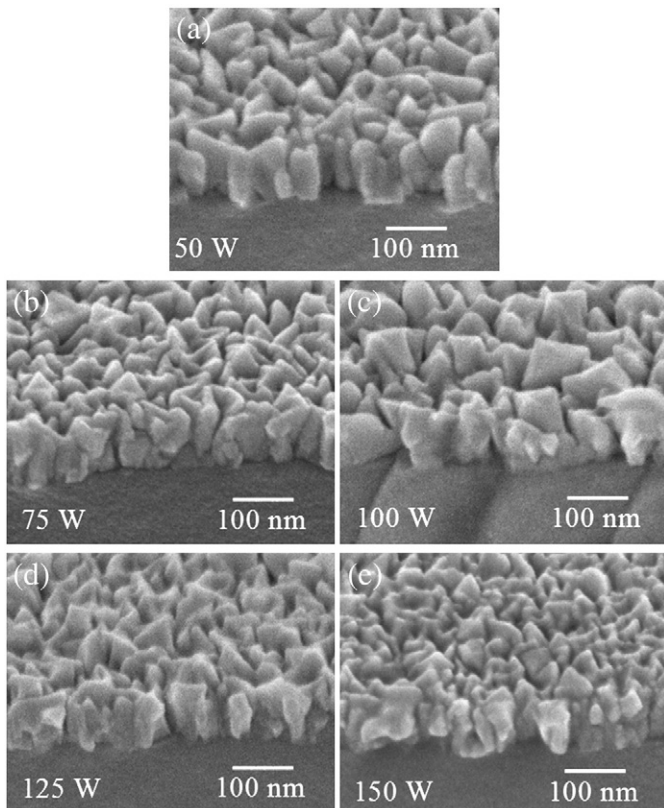


Fig. 3. FESEM photographs of AZO films deposited with RF power of: (a) 50, (b) 75, (c) 100, (d) 125, and (e) 150 W.

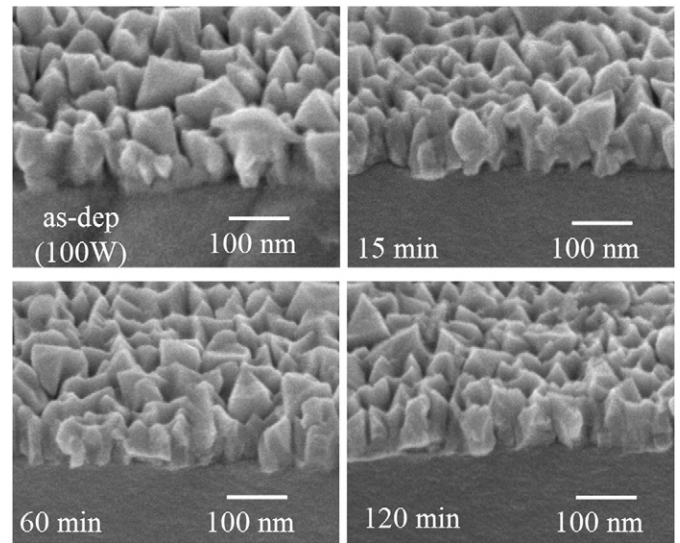


Fig. 4. FESEM photographs of AZO films deposited at RF power of 100 W with or without further plasma treatment at 300 °C for various times.

target. A 13.56 MHz radio-frequency (RF) magnetron sputtering source was set in a chamber to deposit a ceramic thin film. A vacuum system with a base pressure of 5×10^{-6} Torr was used for deposition process. Coning 1737 glass was used as a substrate, which was cleaned with isopropyl alcohol (IPA) and deionized (DI) water, and dried under a flowing nitrogen gas. The AZO films were deposited on glass substrates, which were rotated at 40 rpm, at a temperature of 300 °C using reactive RF magnetron sputtering. Sputtering was carried out at a pressure of 5×10^{-2} Torr in argon (99.99%) gas with RF power of 50–150 W. The film thickness was about 100 nm. After deposition, the AZO thin films were post-treated under hydrogen plasma using a PECVD system at RF power of 10 W for 15, 30, 60, 90 and 120 min and at a substrate temperature of 300 °C. Film thickness was determined by a spectroscopic ellipsometer (SE, MF-1000, Korea). The structure of the AZO films was examined by an X-ray diffractometer (XRD)

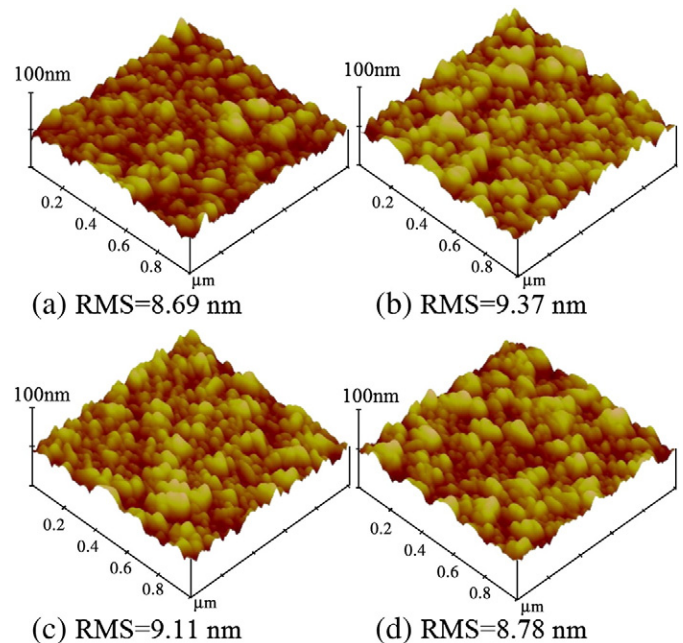


Fig. 5. AFM images of AZO films over $1 \mu\text{m} \times 1 \mu\text{m}$ area: (a) as-deposited and plasma treatment at 300 °C for (b) 30, (c) 60, and (d) 90 min.

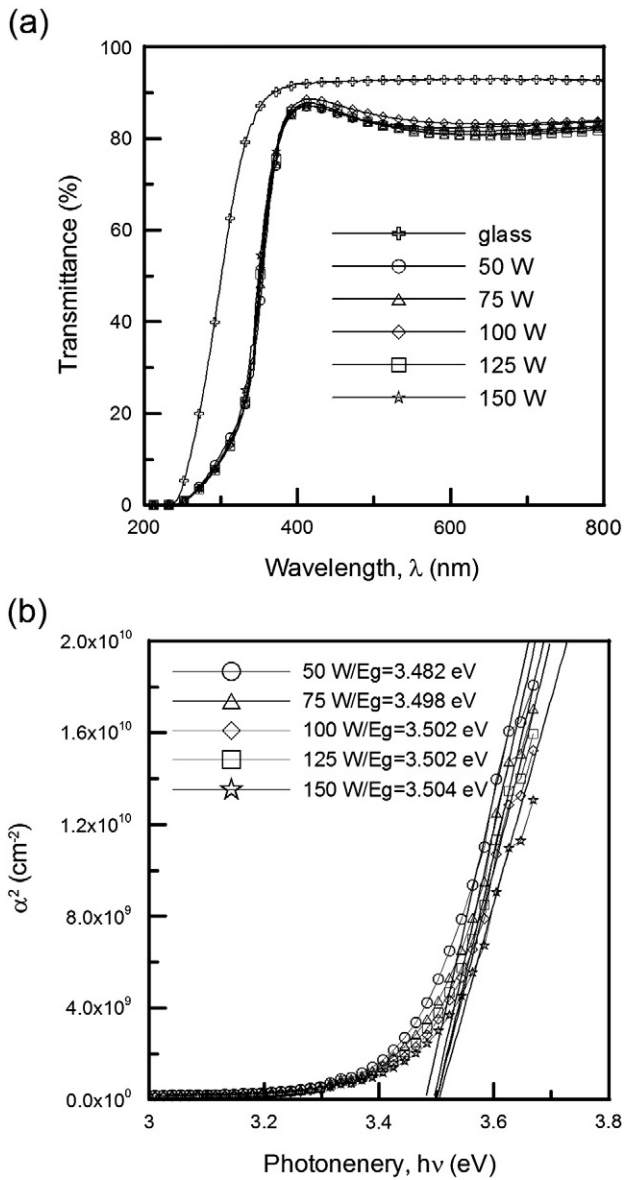


Fig. 6. (a) Optical transmittance and (b) α^2 vs. photon energy ($h\nu$) of AZO films deposited at different RF power. (b) α^2 vs. photon energy ($h\nu$) of AZO films deposited at different RF power.

(PANalytical, 18 kW Rotating Anode X-ray Generator, Japan) with Cu-K α radiation ($\lambda=0.154056$ Å). The morphology of the films was observed using a field emission scanning electron microscope (FESEM) (JSM-6700, JEOL, Japan). The surface roughness was measured using an atomic force microscope (AFM) (Digital Instrument, NS4/D3100CL, Germany). The resistivity, Hall mobility and carrier concentration were measured using the four-point probe technique (Napson, RT-70/RG-5, Japan) and the Van der Pauw technique (BIO-RAD, HL5500IU) at room temperature. The optical transmission spectrum was measured using a UV-VIS spectrometer (JASCO, V-570, Japan) in the wavelength ranging from 200 to 800 nm.

3. Results and discussion

Fig. 1(a) shows the XRD spectra of AZO films prepared at RF powers ranging from 50 to 150 W. The results indicated that all of the AZO films had (002) preferred orientation with the c -axis perpendicular to the substrate regardless of the RF power. The (002) peak was

found at $2\theta \sim 34.36^\circ \pm 0.07^\circ$ which was close to that ($2\theta \sim 34.45^\circ$) of the ZnO crystal. The intensity of the (002) peak increased with the sputtering power. Notably, the intensity of (002) diffraction peak decreased when the sputtering power reached to 125 W. As the RF power increased from 50 to 100 W, the surface atoms had increased energy, thus the film crystallinity was improved. As the RF power increased from 100 to 150 W, increased power enhanced high energetic ion bombardment leading to damage and thus deteriorated the crystallinity of the films. The full-width at half-maximum (FWHM) increased with the RF power, indicating that the crystal size of the AZO film decreased as the RF power increased.

Fig. 2(a) shows the XRD spectra of AZO films treated by hydrogen plasma for various times. The (002) peaks of the as-deposited and the plasma-treated samples do not obviously shift. The FWHMs of the (002) peaks were about $0.34^\circ \pm 0.03^\circ$ for all samples. The hydrogen plasma treatment did not noticeably change the structure of the AZO film.

Fig. 3(a)–(e) exhibits the FESEM images of AZO films deposited at various RF power in the range of 50–150 W. Finding showed that all

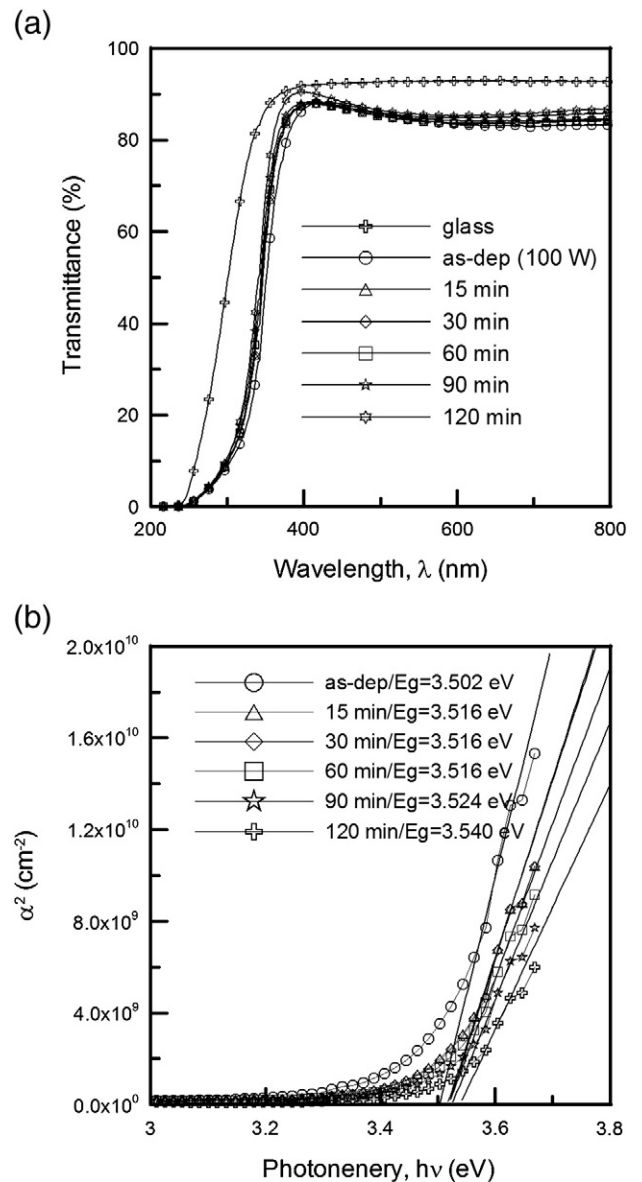


Fig. 7. (a) Optical transmittance and (b) α^2 vs. photon energy ($h\nu$) of AZO films deposited at RF power of 100 W with or without further plasma treatment at 300 °C for various times.

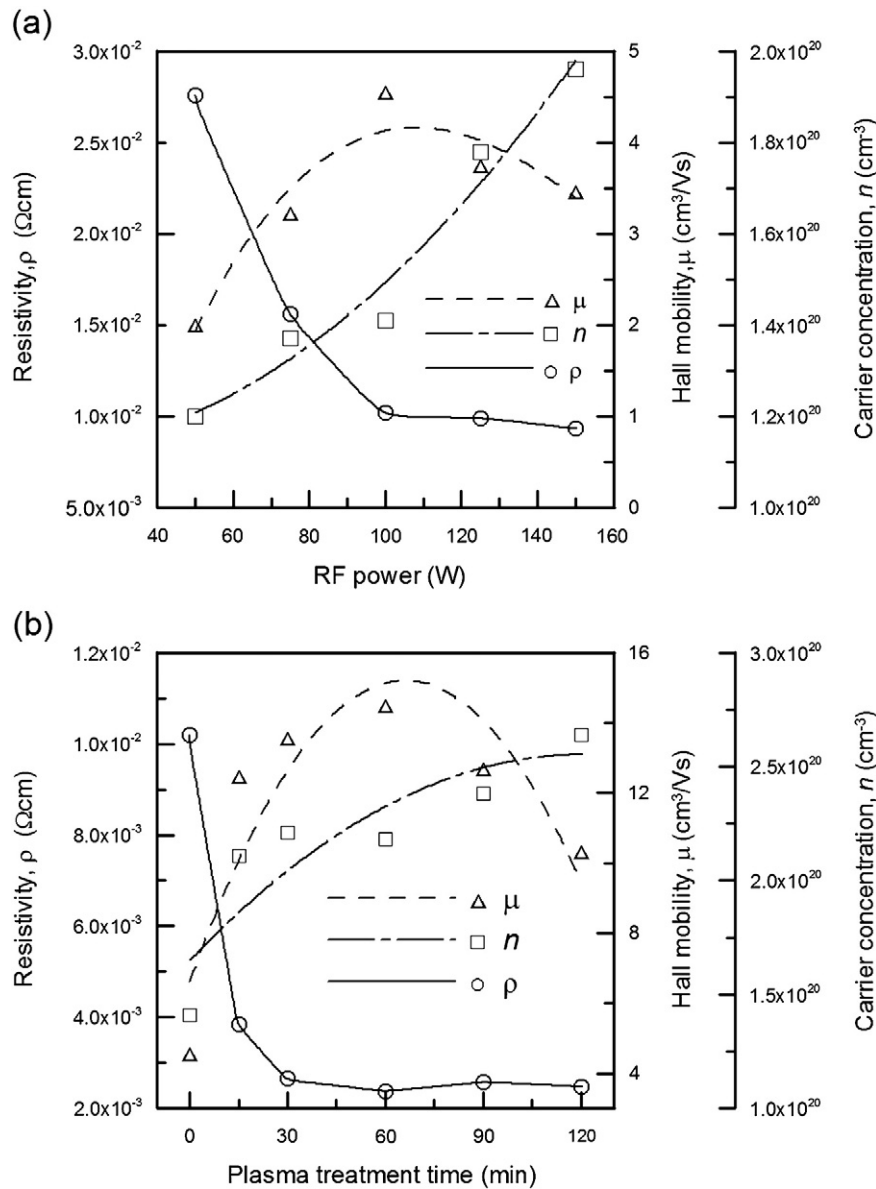


Fig. 8. (a) Electrical resistivity, Hall mobility, and carrier concentration of AZO films deposited at various RF power. (b) Electrical resistivity, Hall mobility, and carrier concentration of AZO films deposited at RF power of 100 W with or without further plasma treatment for various times.

the AZO films had columnar structures despite the sputtering RF power. For lower RF power (50–100 W), the grain size of the AZO film increased with increasing RF power and then achieved the maximum value (about 60–100 nm) at 100 W. The larger grain size is attributed to the higher RF power causing higher substrate temperature and growth rate during sputtering process [18]. However, as the RF power increased above 125 W, the grain size was slightly decreased and some small grains were found due to re-sputtering at high RF power. The trend of grain structure agrees with the results from XRD analysis.

Fig. 4(a)–(d) displays the FESEM images of AZO films treated by hydrogen plasma for 0 (as-deposited), 15, 60, and 120 min. The plasma-treated films had similar grain structure with the as-deposited ones, but some large grains disappeared after plasma treatment. In addition, the results exhibited that grain boundaries were slightly etched for the sample with longer plasma duration (120 min), as shown in Fig. 4(d).

The surface morphology of AZO films was investigated using an AFM. Fig. 5(a)–(d) shows AFM images of the films treated by plasma for 0 (as-deposited), 30, 60, and 90 min. The RMS roughnesses were 8.69, 9.37, 9.11, and 8.78 nm for the films treated for 0, 30, 60, and

90 min, respectively. The surface roughness slightly increased and then decreased after a 60-min plasma treatment due to the etching effect of hydrogen plasma. The small variations in the surface roughness of the plasma-treated films were attributed to small RF power during plasma treatment.

Fig. 6(a) shows the optical transmittances of AZO films deposited at various RF power. The average transmittances in the visible range (400–700 nm) were 83.1%, 82.8%, 85.0%, 82.8% and 83.6% for RF power of 50, 75, 100, 125 and 150 W, respectively. Dependence of optical absorption coefficient (α) on photon energy ($h\nu$) was examined to determine optical bandgap energy (E_g) of the AZO films. Fig. 6(b) shows the plot of α^2 against $h\nu$ to obtain E_g of the films, and the sharp absorption edge can be accurately determined by linear fitting [19]. The optical bandgap of the AZO film widened from 3.482 to 3.504 eV as the RF power increased from 50 to 150 W. The blue shift of the bandgap is explained by the Burstein–Moss (BM) shift [20].

Fig. 7(a) and (b) shows the optical transmittances and bandgaps, respectively, for the AZO films prepared at 100 W and treated by hydrogen plasma for different exposure time. The average transmittances in the visible region (400–700 nm) were 85.0%, 85.3%, 85.0%,

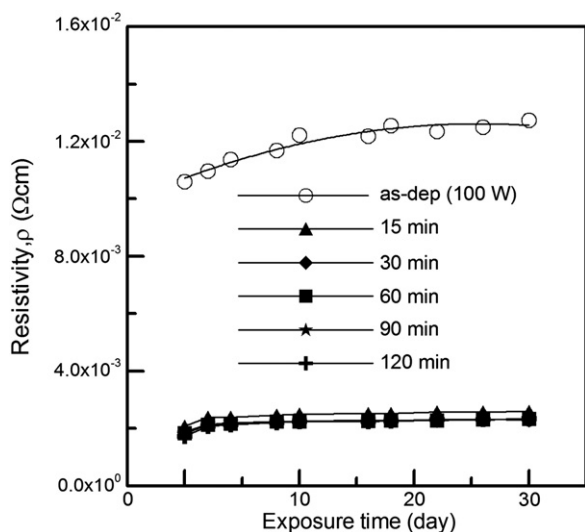


Fig. 9. Electrical stability of the as-deposited and plasma-treated AZO films aged in air at room temperature.

84.9%, 85.8% and 86.5% for plasma time of 0 (as-deposited), 15, 30, 60, 90 and 120 min, respectively. The transmittance of the plasma-treated films did not markedly vary with increasing plasma exposure time. From Fig. 7(b), the bandgaps coherently broadened from 3.504 to 3.540 eV with increasing hydrogen plasma treatment time. The blue-shift of the absorption edge is attributed to the above-mentioned BM effect.

Fig. 8(a) shows the dependence of electrical resistivity (ρ), Hall mobility (μ), and carrier concentration (n) of AZO films on various RF power. Results indicated the film resistivity decreased with the increase of RF power. The lowest resistivity was $9.30 \times 10^{-3} \Omega \text{ cm}$ at a power of 150 W. The carrier concentration of the AZO films increased from 1.20×10^{20} to $1.96 \times 10^{20} \text{ cm}^{-3}$ as the RF power increased from 50 to 150 W. The result of increased carrier concentration agrees with the blue-shift on the optical bandgap. The Hall mobility increased and then decreased as the RF power increased from 50 to 150 W. The optimal Hall mobility was $4.55 \text{ cm}^2/\text{Vs}$ at RF power of 100 W. The reduced Hall mobility results from small grain size and poor crystal quality, as the results of the FESEM and XRD analyses indicate. Fig. 8(b) shows the electrical resistivity, Hall mobility and carrier concentration of AZO films as a function of plasma treatment time. The carrier concentration increased from 1.41×10^{20} to $2.64 \times 10^{20} \text{ cm}^{-3}$ as the hydrogen plasma treatment time increased to 120 min. The Hall mobility increased from 4.5 to $14.6 \text{ cm}^2/\text{Vs}$ as the plasma time increased from 0 to 60 min and then decreased to $10.3 \text{ cm}^2/\text{Vs}$ as the plasma time increased to 120 min. The appropriate hydrogen plasma treatment effectively improves carrier concentration and Hall mobility, leading to the reduction of film resistivity. The electrical resistivity of the plasma-treated AZO film decreased from 1.02×10^{-2} to $2.38 \times 10^{-3} \Omega \text{ cm}$ after a 60-min plasma treatment. A significant decrease in film resistivity may be achieved due to the removal of weakly bound oxygen species on the grain boundaries [15]. Loss of oxygen from the crystal will also produce the interstitial Zn atoms, thus increasing carrier concentration and decreasing film resistivity [12]. Additionally, the adsorbed hydrogen atoms in plasma-treated films may form Zn-H type species and

generate free electrons, thus further decreasing the resistivity [21,22].

Fig. 9 shows the electrical stability of the as-deposited and plasma-treated AZO films aged in air at room temperature. After exposing to air atmosphere for 30 days, the increment of the film resistivity for the as-deposited sample was much larger than that for the plasma-treated ones even though the plasma treatment time was only 15 min. The improved electrical stability may be attributed to fewer weakly bound oxygen species in the hydrogen plasma-treated films and more deep-level defects passivated with strong bonds than the as-deposited ones with air exposure. This work concluded that hydrogen plasma treatment could effectively improve the electrical property of AZO films and enhance their stability [14,23,24].

4. Conclusions

Transparent conductive AZO films have been deposited on glass substrates by RF magnetron sputtering at varying RF power ranging from 50 to 150 W and treated by hydrogen plasma at 300°C in a PECVD system. The AZO film achieved a maximum grain size of about 60–100 nm at an RF power of 100 W. The hydrogen plasma treatment effectively improved the electrical characteristics of the AZO films, but did not noticeably change the structure of the AZO film. The film resistivity decreased from 1.02×10^{-2} to $2.38 \times 10^{-3} \Omega \text{ cm}$ after a 60-min plasma treatment. The optical bandgap increased from 3.504 to 3.540 eV, as the plasma exposure time increased from 0 to 120 min. After the hydrogen plasma treatment, the electrical stability of the AZO films aged in air was also improved.

Acknowledgment

This work was partially supported by the National Science Council of ROC (Taiwan) under contract no. NSC 95-2221-E-005-111.

References

- [1] T. Minami, H. Nanto, S. Takata, *Jpn. J. Appl. Phys.* 23 (1984) L280.
- [2] T. Minami, H. Sato, H. Nanto, S. Takata, *Jpn. J. Appl. Phys.* 24 (1985) L781.
- [3] T. Minami, H. Sato, H. Nanto, S. Takata, *Thin Solid Films* 176 (1989) 277.
- [4] P.L. Almeida, M.H. Godinho, M.T. Cidade, P. Nunes, A. Marques, R. Martins, E. Fortunato, J.L. Figueirinhas, *Synth. Met.* 127 (2002) 111.
- [5] S.H. Yoon, J.S. Kim, Y.S. Kim, *Curr. Appl. Phys.* 6S1 (2006) e154.
- [6] H. Kim, J.S. Horwitz, W.H. Kim, A.J. Makinen, Z.H. Kafafi, D.B. Chrisey, *Thin Solid Films* 420/421 (2002) 539.
- [7] V. Sittinger, F. Ruske, W. Werner, B. Szyszka, B. Rech, J. Hupkes, G. Schöpe, H. Stiebig, *Thin Solid Films* 496 (2006) 16.
- [8] H. Zhu, E. Bunte, J. Hüpkes, H. Siekmann, S.M. Huang, *Thin Solid Films* 517 (2009) 3161.
- [9] S.S. Lin, J.L. Huang, P. Sajgalik, *Surf. Coat. Technol.* 190 (2005) 39.
- [10] G. Blaustein, M.S. Castro, C.M. Aldao, *Sens. Actuators, B* 55 (1999) 33.
- [11] C.G. Van de Walle, J. Neugebauer, *Nature* 423 (5) (2003) 626.
- [12] G. Fang, D. Li, B.L. Yao, *Vacuum* 68 (2003) 363.
- [13] B.Y. Oh, M.C. Jeong, D.S. Kim, W. Lee, J.M. Myoung, *J. Cryst. Growth* 281 (2005) 475.
- [14] Y.M. Chung, C.S. Moon, W.S. Jung, J.G. Han, *Thin Solid Films* 515 (2006) 567.
- [15] B.Y. Oh, M.C. Jeong, J.M. Myoung, *Appl. Surf. Sci.* 253 (2007) 7157.
- [16] R. Das, T. Jana, S. Ray, *Sol. Energy Mater. Sol. Cells* 86 (2005) 207.
- [17] N. Ohashi, Y.G. Wang, T. Ishigaki, Y. Wada, H. Taguchi, I. Sakaguchi, T. Ohgaki, Y. Adachi, H. Haneda, *J. Cryst. Growth* 306 (2007) 316.
- [18] N.H. Kim, H.W. Kim, *Mater. Lett.* 58 (2004) 938.
- [19] O. Hamad, G. Braunstein, H. Patil, N. Dhere, *Thin Solid Films* 489 (2005) 303.
- [20] B.E. Sernelius, K.F. Berggren, Z.C. Jim, I. Hamberg, C.G. Granqvist, *Phys. Rev. B* 37 (1988) 10244.
- [21] C.G. Van de Walle, *Phys. Rev. Lett.* 85 (2000) 1012.
- [22] J.M. Lee, K.K. Kim, S.J. Park, W.K. Choi, *Appl. Phys. Lett.* 78 (2001) 3842.
- [23] S.J. Baik, J.H. Jang, C.H. Lee, W.Y. Cho, K.S. Lim, *Appl. Phys. Lett.* 70 (1997) 3516.
- [24] Y.S. Kang, H.Y. Kim, J.Y. Lee, *J. Electrochem. Soc.* 147 (2000) 4625.